Propagation in Dielectric-Lined Square Waveguides

G. N. TSANDOULAS, MEMBER, IEEE

Abstract—**Symmetric structures such as circular and square waveguides may conveniently be used for dual polarization application. In this work the square waveguide with a dielectric lining of the same geometry is analyzed using a Galerkin-type method, with experimental verification. Modal characteristics, propagation constants, and bandwidth (BW) properties are outlined. Some interesting variations, depending on whether the value of the dielectric constant of the lining is higher or lower than that of the included material, are described and quantified to the extent possible by the accuracy of the method.**

INTRODUCTION

INHOMOGENEOUSLY loaded waveguides have found wide application in many microwave disciplines including electronic phase shifting [1], [2] and aperture control [3], [4]. More recently, the square shape has received attention because it is of interest in a number of applications, including phased arrays. In the latter case, square waveguides have been shown to be viable radiators for dual polarization and for bandwidths (BW's) of up to 25 percent of center frequency [5]. By contrast, circular waveguides possess more severe modal BW constraints which appear to limit their practical-design BW capability to about 17 percent of center frequency, at least for the phased-array application. In a recent development [6], an accurate computation was obtained of the modal (TE_{11}–TM_{01}) BW enhancement in dielectric-lined circular waveguide. Therefore, the possibility of obtaining a similar improvement with dielectric-lined square waveguide was a logical hypothesis.

Apart from the interest in BW,[1] other applications necessitate knowledge of the propagation characteristics of this structure. The improvement in horn aperture efficiency obtained with E-plane dielectric slabs [3] or in pattern control with either E-plane [3] or H-plane [4] slabs has led to the suggestion [3] that such effects might still be possible with both E-plane and H-plane slabs (i.e., dielectric lining) in a square waveguide for applications requiring circular polarization. The theory is also applicable to the optimization of square Faraday rotators [7] and to configurations used in the velocity modulation of pulsed electron beams and large aperture microwave electrooptic modulators [8], to mention but a few practical cases. From a theoretical standpoint a comparison of such idiosyncratic peculiarities as model inversion [1], [6], [9], and backward waves [10], [11] with their counterparts in the circular waveguide case should be of interest in understanding the varied EM response of two essentially similar geometrical structures.

Manuscript received September 12, 1974; revised December 23, 1974. This work was sponsored by the Department of the Army.

The author is with the Massachusetts Institute of Technology, Lincoln Laboratory, Lexington, Mass. 02173.

[1] Wide instantaneous BW in a radar system is necessary for enhanced range resolution among other things.

ANALYSIS

The structure under investigation is shown in Fig. 1. Two cases are distinguished according to whether the dielectric lining has a higher dielectric constant than the core material or vice versa. In the figure, ϵ_1 and ϵ_2 are the values of the dielectric constants relative to free space. ϵ_r is used to designate the ratio ϵ_1/ϵ_2 for Fig. 1(a) or the ratio ϵ_2/ϵ_1 for Fig. 1(b) throughout this work.

In deciding upon the method of analysis, priority was given to techniques which are as inclusive as possible in the sense that they will allow for the solution of a wide class of problems with little additional formulational labor, once the basic mathematical formalism has been properly laid out. In this sense, a Galerkin-type procedure due to Baier [12] was selected as promising. Briefly, it works as follows. An arbitrary transverse variation

$$\epsilon = \epsilon\,(x,y) \tag{1}$$

is assumed for the relative (to free space) dielectric constant in a lossless rectangular waveguide of width a and height b, while no changes in the magnetic properties are allowed (that is, $\mu_r = 1$ where μ_r is the magnetic permeability relative to free space). Under the gauge

$$\Phi = \frac{j\nabla \cdot A}{\omega\epsilon_0\epsilon} \tag{2}$$

for the static potential Φ and the H-related vector potential A, Maxwell's source-free equations lead to two coupled second-order differential equations for the two components A_x and A_y in which the relative dielectric constant $\epsilon\,(x,y)$ appears only in the form $1/\epsilon$ and $\nabla(1/\epsilon)$. Assuming the trigonometric series expansions

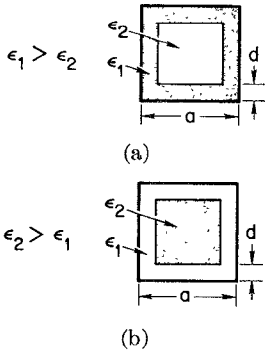

Fig. 1. Transverse geometry of the dielectric-lined square waveguide.

$$A_x = \sum_{m,n} X_{mn} L_{mn} \tag{3}$$

$$A_y = \sum_{m,n} Y_{mn} L_{mn} \tag{4}$$

$$\epsilon^{-1} = \sum_{p,q} K_{pq} L_{pq} \tag{5}$$

where

$$L_{rs} = \exp j\left(\frac{r\pi x}{a} + \frac{s\pi y}{b}\right), \qquad r = m,p;\ s = n,q$$

and where the summations are from $-\infty$ to $+\infty$, the equations may be put into a matrix configuration with the eigenvectors X_{mn} and Y_{mn} as the unknowns and the eigenvalues (i.e., the characteristic frequencies) determined by the usual eigenvalue matrix inversion operations.

The Fourier coefficients K_{pq} are determined from

$$K_{pq} = (ab)^{-1} \iint_A \epsilon^{-1} \cos\frac{\pi px}{a} \cos\frac{\pi qy}{b}\, dxdy \tag{6}$$

integrated over the waveguide cross-section area. It is this last feature that makes this particular technique attractive. The K_{pq} for very general and complicated geometrical configurations may easily be computed since a closed form is not really necessary for computer calculations. Then any particular subgeometry is solved simply by specifying its geometrical parameters without any additional effort. In our case such a problem was indeed set up and the K_{pq} were determined. The dielectric-lined square guide constitutes a special case with the following expansion coefficients:

$$K_{00} = \frac{1}{\epsilon_1} + \left(\frac{1}{\epsilon_2} - \frac{1}{\epsilon_1}\right)\left(1 - 2\frac{d}{a}\right)^2 \tag{7a}$$

$$K_{pq} = 0 \text{ for either } p = \text{odd or } q = \text{odd} \tag{7b}$$

$$K_{p0} = -2\left(\frac{1}{\epsilon_2} - \frac{1}{\epsilon_1}\right)\left(1 - 2\frac{d}{a}\right)\frac{\sin \pi p(d/a)}{\pi p} \tag{7c}$$

$$K_{0q} = \text{same as } K_{p0} \text{ with } q \text{ replacing } p$$

$$K_{pq} = 4\left(\frac{1}{\epsilon_2} - \frac{1}{\epsilon_1}\right)\frac{\sin \pi p(d/a)}{\pi p}\,\frac{\sin \pi q(d/a)}{\pi q}$$

$$\text{for } p \text{ and } q \neq 0. \tag{7d}$$

Although this procedure gives great flexibility in problem solving, it is based on the method of moments, and as such it must be carefully scrutinized as to degree of convergence. This depends on the parameters of the particular geometry such as filling factors and dielectric constants. For the problem under consideration, the most crucial parameter is the ratio $\epsilon_r (= \epsilon_1/\epsilon_2 \text{ or } \epsilon_2/\epsilon_1)$. Fig. 2 shows convergence as a function of eigenvalue matrix size. It is clear that large computation times are necessary for the high ϵ_r cases even when advantage is taken of symmetry, as suggested by Baier [12], to reduce the amount of stored data. In the computations that follow, the eigenvalue matrix size was chosen so as to give an estimated worst case eigenvalue accuracy in the neighborhood of 2 percent for ϵ_r ratios up to about 10, determined by criteria such as the plot of Fig. 2. The method yields all the eigenvalues at once but two different matrix relations must be solved, one for the TE_{mn} (more properly HE_{mn}) and another for the TM_{mn} (more properly EH_{mn}) modes. Convergence is monotonic so that the apparent oscillation in Fig. 2 is really a change in the rapidity (slope) of convergence and does not represent oscillatory behavior for the eigenvalue itself.

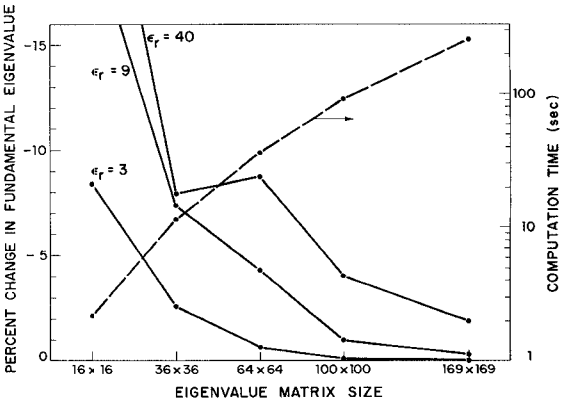

Fig. 2. Convergence of the fundamental-mode eigenvalue for the structure of Fig. 1(a) with $d/a = 0.15$ (IBM 360/67 computer).

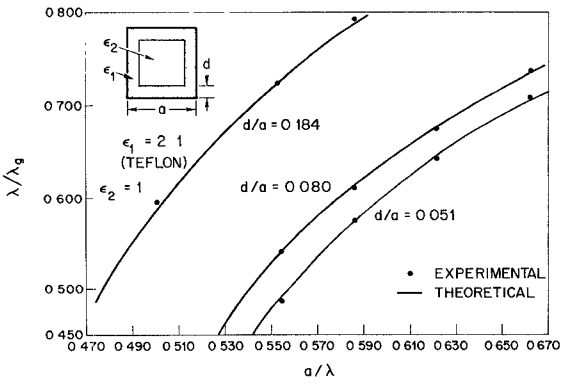

Fig. 3. Theoretical and experimental determination of the normalized fundamental-mode propagation constant λ_g showing excellent agreement. Measurements were made at C band (5.65-GHz center frequency). λ is the free-space wavelength.

Two types of accuracy checks were applied to the solutions. First, some standard and well-known problems were solved and the answers compared with published or already existing solutions [13]. Exactly solvable geometries, such as multiple dielectric slabs [14], were also treated successfully. As expected, for equal accuracy, smaller matrices were required for the exactly solvable geometries for which either A_x or A_y vanishes than for the equivalently loaded nonseparable ones for which both A_x and A_y are nonzero. The second test was an experimental determination of the propagation constant in a few special cases of the dielectric-lined square waveguide. The agreement between theory and experiment is shown in Fig. 3. A long section of guide was prepared and tested at C band by determining the standing-wave pattern at various points along the guide. Access to the interior was achieved through the use of small holes through

which a probe was inserted. It was found that objectionable amounts of radiation resulted with a longitudinally slotted guide, hence the switch to small coupling holes.

RESULTS

The variation of the propagation constant with frequency for the case $\epsilon_1 > \epsilon_2$ is shown in Figs. 4 and 5 for two common materials, Teflon ($\epsilon_r = 2.1$) and nylon ($\epsilon_r = 3.0$). Although all the modes of the structure are hybrid, the TE and TM nomenclature has been preserved to identify the modes according to their character in the limiting case of the fully filled ($d/a = 0.5$) or empty ($d/a = 0$) guide. Accordingly, Fig. 6 shows cutoff distributions for some of the modes. It is interesting to compare how the TE_{11}–TM_{11} and TE_{21}–TM_{21} cutoff degeneracies are lifted by the dielectric discontinuity. Almost no splitting is noticed for the first pair although the splitting widens for the higher ϵ_r cases. The second pair separates at the outset, its more complex field line structure being more sensitive to the transverse change in the dielectric medium. This applies also to all higher order cutoff degeneracies. Another feature of interest in Fig. 6 is the reordering of the modal hierarchy for certain ranges of the filling factor d/a. Thus the TE_{20} mode is quickly superseded, first by the TM_{21} mode (this inversion begins at $\epsilon_1/\epsilon_2 \approx 2.0$) and, as ϵ_r increases, by the TE_{21} and other higher modes. The BW characteristics are shown in Fig. 7. In contrast to the dielectric-lined circular waveguide, modal BW is always less than or equal to the empty-guide value. BW is computed according to the formula

$$\text{BW (percent)} = 200\left[\frac{f_{c+} - f_{c-}}{f_{c+} + f_{c-}}\right] \tag{8}$$

where f_{c-} is the cutoff frequency of the lowest mode and f_{c+} is the cutoff frequency of the first higher order mode.

One of the most important features of the mode structure for Fig. 1(a) is the fact that the TE_{10} mode remains fundamental throughout the entire range of dielectric constants and filling factors. No such property is maintained for the dielectrically loaded case [Fig. 1(b)]. Modal separation begins to shrink (Fig. 8) with the result that at an ϵ_r value very close to 10, a value of d/a ($\simeq 0.28$) exists at which the first two modes are cutoff degenerate. Any further increase in ϵ_r enlarges the region of modal inversion and a "negative" BW is obtained (Fig. 9). Concurrently, a backward-wave region begins to form for the initially dominant mode, much the same way it develops for the circular waveguide case [9], [10]. No attempt was made to determine more accurately the onset of the cutoff degeneracy. However, it must surely be related to the onset of ambiguity in circular waveguides, for which the critical value of ϵ_r has been variously estimated as $\epsilon_{r_c} = 9.37$ [11], $\epsilon_{r_c} = 10.5$ [15], and, more recently, $\epsilon_{r_c} = 9.13$ [16]. The spread of values gives an idea of the difficulty of obtaining an accurate figure even for the exactly solvable geometry of the circular waveguide.

Computer-provided field lines for a typical, fundamental-

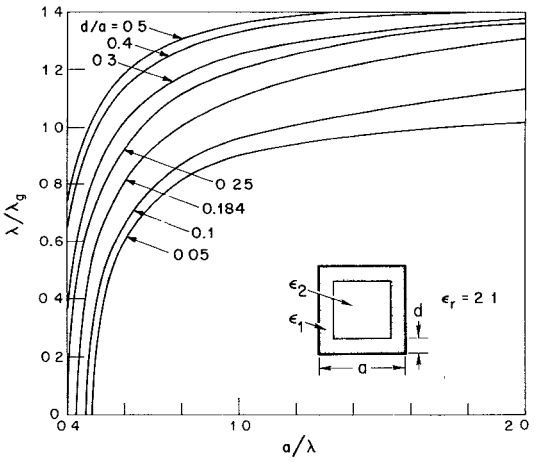

Fig. 4. Propagation-constant variation with frequency for Teflon-lined square waveguide.

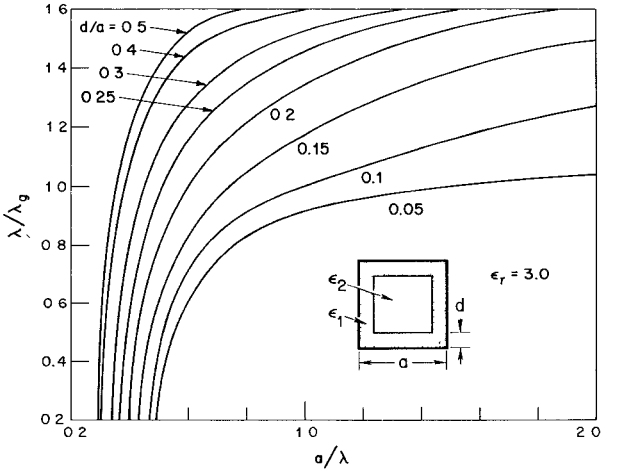

Fig. 5. Propagation-constant variation with frequency for nylon-lined square waveguide.

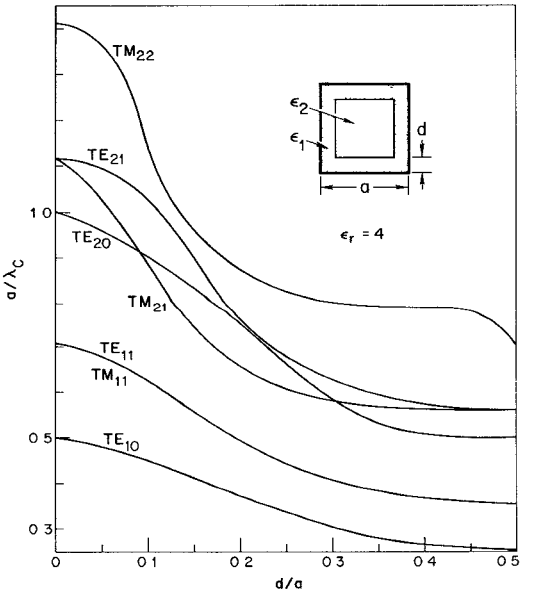

Fig. 6. Cutoff-wavelength (λ_c) variation versus filling factor for some of the first few modes for Fig. 1(a).

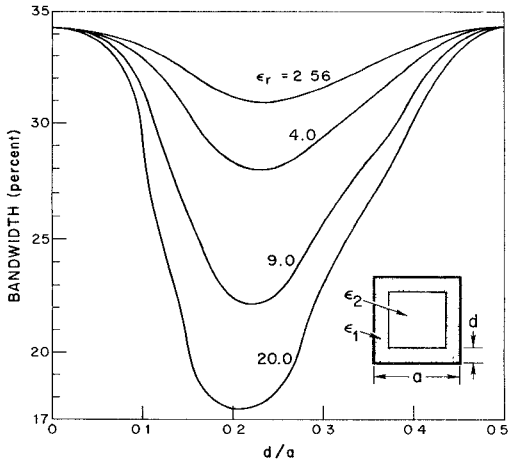

Fig. 7. Modal-BW variation with filling factor for Fig. 1(a). BW definition is given in (8).

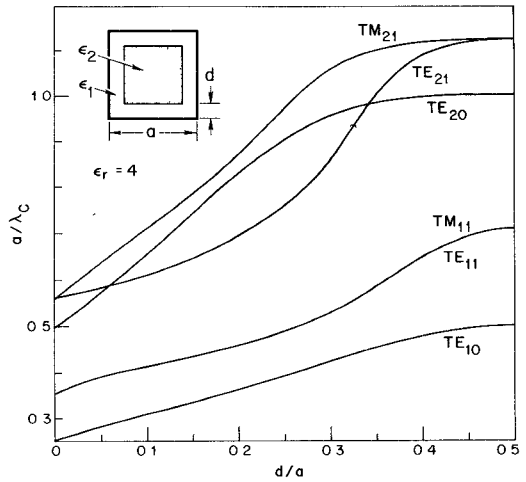

Fig. 8. Cutoff-wavelength (λ_c) variation versus filling factor for some of the first few modes for Fig. 1(b).

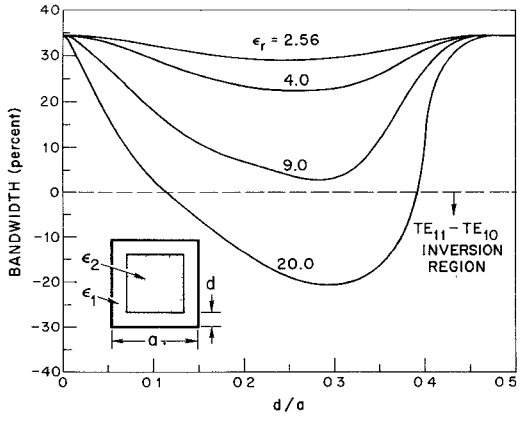

Fig. 9. Modal-BW variation with filling factor for Fig. 1(b) showing inversion property. BW definition is given in (8).

mode configuration are shown in Fig. 10. The lines are really three-dimensional so that only the transverse components are involved in Fig. 10. In Fig. 11, the loci of the first cutoff degeneracy for the dielectric-lined case and of the first and second cutoff degeneracies for the dielectric-loaded case have been plotted in the ϵ_r, d/a plane. As far as can be ascertained by the solutions, the TE_{20} degeneracy begins at the same value of ϵ_r ($\approx$2.0) for both cases and at approximately the same filling factor, although the steepness of the slope at that point precludes a more exact determination.

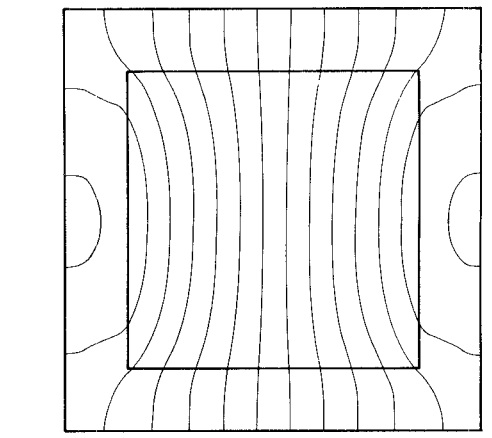

Fig. 10. Momentary electric displacement lines for the fundamental mode of Fig. 1(b). Parameters are $\epsilon_r = 4$, $d/a = 0.15$, $a/\lambda = 1.0$.

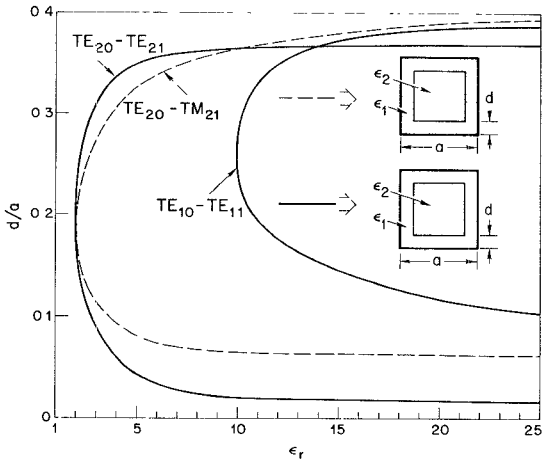

Fig. 11. Cutoff degeneracy manifolds in the ϵ_r, d/a plane for three-mode pairs.

CONCLUSION

Although many interesting properties of the dielectric-lined square waveguide were investigated, the primary concern has been with bandwidth. It was shown that for both cases of Fig. 1 BW decreases with loading, never rising above the fully filled waveguide case. In this respect the dielectric-lined circular waveguide can be almost as wide band [6] as the fully filled square waveguide.

It would be of interest to summarize BW comparison in circular and square structures. This is shown in Fig. 12 for both lined and ridged circular and square waveguides. For the circular cases, a parameter selection leading to maximum or near maximum available BW was made. From the figure it is evident that the double-ridged circular waveguide has inherently greater BW with very good dual

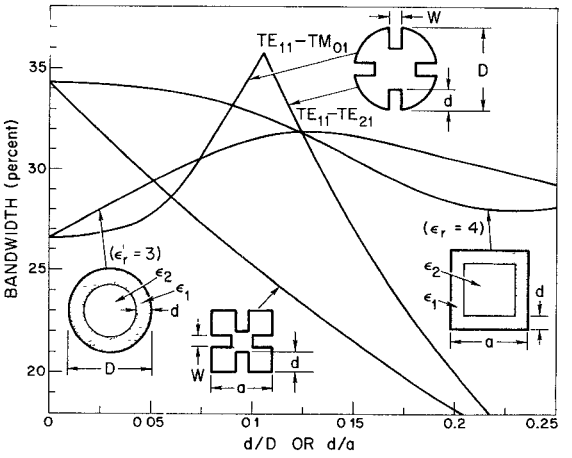

Fig. 12. A contrast of the BW properties of four waveguide types suitable for dual polarization applications. Results were taken from the following sources: Dielectric-lined square waveguide (this paper), dielectric-lined circular waveguide [6], double-ridged square and circular waveguides [17] with $W/a = W/D = 0.15$).

polarization capability. Some experimentation is presently in the planning stage to ascertain antenna pattern quality for the two independent linearly polarized modes (TE_{10}–TE_{01}) with a dielectric-lined square waveguide.

As was mentioned earlier, the chosen method of solution permits the investigation of a large number of subgeometries, once the coefficients for a very general problem have been defined. This was especially useful in the present case for a very particular reason. One may notice from Fig. 12 that ridged and dielectric-lined square waveguides have reduced BW properties. Also, no increase in BW was observed for a number of configurations in which the transverse dielectric distribution was varied by suitable parameter choice, albeit always in a symmetrical manner. The hypothesis is therefore advanced that inhomogeneous but symmetric dielectric loading of square waveguides will invariably reduce modal BW. The plausibility of this statement becomes more evident if one examines the field lines for the TE_{10} and TE_{11} modes in the unloaded square waveguide. It is very difficult to configure a loading scheme that will take advantage of field distribution differences so that truly differential loading favoring the TE_{10} mode will result. This type of loading is necessary for BW increase. By contrast, the TE_{11} and TM_{01} modes of the circular waveguide possess enough diversity so that differential loading of the TE_{11} mode by dielectric lining may yield larger BW.

ACKNOWLEDGMENT

The author wishes to thank F. Willwerth for carrying out the experimental measurements.

REFERENCES

[1] G. N. Tsandoulas and W. J. Ince, "Modal inversion in circular waveguides—Part I: Theory and phenomenology; Part II: Application to latching nonreciprocal phasers," *IEEE Trans. Microwave Theory Tech.*, vol. MTT-19, pp. 386–400, Apr. 1971.

[2] W. J. Ince and E. Stern, "Nonreciprocal remanence phase shifters in rectangular waveguide," *IEEE Trans. Microwave Theory Tech.*, vol. MTT-15, pp. 87–95, Feb. 1967.

[3] G. N. Tsandoulas and W. D. Fitzgerald, "Aperture efficiency enhancement in dielectrically loaded horns," *IEEE Trans. Antennas Propagat.*, vol. AP-20, pp. 69–74, Jan. 1972.

[4] R. Baldwin and P. A. McInnes, "Radiation patterns of dielectric loaded rectangular horns," *IEEE Trans. Antennas Propagat.* (Commun.), vol. AP-21, pp. 375–376, May 1973.

[5] G. N. Tsandoulas and G. H. Knittel, "The analysis and design of dual-polarization square-waveguide phased arrays," *IEEE Antennas Propagat.*, vol. AP-21, pp. 796–808, Nov. 1973.

[6] G. N. Tsandoulas, "Bandwidth enhancement in dielectric-lined circular waveguides," *IEEE Trans. Microwave Theory Tech.* (Corresp.), vol. MTT-21, pp. 651–654, Oct. 1973.

[7] H. C. Bell, Jr., and C. R. Boyd, Jr., "Optimum filling of ferrite phase shifters of uniform dielectric constant," *IEEE Trans. Microwave Theory Tech.*, vol. MTT-22, pp. 360–364, Apr. 1974.

[8] R. G. Heeren and J. R. Baird, "An inhomogeneously filled rectangular waveguide capable of supporting TEM propagation," *IEEE Trans. Microwave Theory Tech.* (Corresp.), vol. MTT-19, pp. 884–885, Nov. 1971.

[9] R. A. Waldron, "Theory and potential applications of backward waves in non-periodic inhomogeneous waveguides," *Proc. Inst. Elec. Eng.*, vol. 111, pp. 1659–1667, Oct. 1969.

[10] P. J. B. Clarricoats and R. A. Waldron, "Non-periodic slow wave and backward wave structures," *J. Electron. Contr.*, vol. 8, pp. 455–458, 1960.

[11] P. J. B. Clarricoats, "Backward waveguides containing dielectrics," *Proc. Inst. Elec. Eng.*, Monograph 451E, vol. 108C, pp. 496–501, June 1961.

[12] W. Baier, "Waves and evanescent fields in rectangular waveguides filled with a transversely inhomogeneous dielectric," *IEEE Trans. Microwave Theory Tech.*, vol. MTT-18, pp. 696–705, Oct. 1970.

[13] W. Schlösser and H. G. Unger, "Partially filled waveguides and surface waveguides of rectangular cross-section," in *Advances in Microwaves*, vol. 1, L. Young, Ed. New York: Academic, 1966, pp. 319–387.

[14] F. E. Gardiol, "Higher-order modes in dielectrically loaded rectangular waveguides," *IEEE Trans. Microwave Theory Tech.*, vol. MTT-16, pp. 919–924, Nov. 1968.

[15] V. Ya. Smorgonskiy, "Calculation of the double-valued part of the dispersion curve of a circular waveguide with dielectric rod," *Radio Eng. Electron. Phys.* (USSR), vol. 13, pp. 1809–1810, 1968.

[16] Yu. A. Ilarionov, "Ambiguity in the dispersion curves of waves of a circular, partially-filled waveguide," *Isv. Vuz, Radioelektron.* vol. 16, pp. 30–37, 1973.

[17] M. H. Chen, G. N. Tsandoulas, and F. G. Willwerth, "Modal characteristics of quadruple-ridged circular and square waveguides," *IEEE Trans. Microwave Theory Tech.*, vol. MTT-22, pp. 801–804, Aug. 1974.